

Optimized Segmentation of Cellular Tomography through Organelles' Morphology and Image Features

Nur Intan Raihana Ruhaiyem, Ahmad Sufri Azlan Mohamed, Bahari Belaton
*Universiti Sains Malaysia,
11800 USM Penang, Malaysia.
intanraihana@usm.my*

Abstract— Computational tracing of cellular images generally requires painstaking job in optimizing parameter(s). By incorporating prior knowledge about the organelle's morphology and image features, the required number of parameter tweaking can be reduced substantially. In practical applications, however, the general organelles' features are often known in advance, yet the actual organelles' morphology is not elaborated. Two primary contributions of this paper are firstly the classification of insulin granules based on its image features and morphology for accurate segmentation – mainly focused at pre-processing image segmentation and secondly the new hybrid meshing quantification is presented. The method proposed in this study is validated on a set of manually defined ground truths. The study of insulin granules in particular; the location, and its image features has also opened up other options for future studies.

Index Terms— Cellular tomography; Organelles' morphology; Image features; Classification of insulin granules.

I. INTRODUCTION

The insulin secretory pathway comprises a series of steps that involves a number of functionally distinct membrane-bound organelles which include the Golgi apparatus, mitochondria, insulin granules, lysosomes, the endoplasmic reticulum (ER) and vesicles. In general, there are two different patterns of secretion. One pattern is referred to as regulated secretion, as proteins are continuously secreted from the cell regardless of environmental factors. No external signals are required to initiate this process. The second pattern is referred to as constitutive secretion for which an external signal is required before secretion occurs. Mature granules represent the beta cells' which act as storage sites for the vast reserves of insulin produced. A typical unstimulated mouse beta cell contains approximately 10,000 mature granules [1]; each measures approximately 200-300 nm in diameter [2] and contains 150,000-280,000 insulin molecules [3]. Mature granules represent different pools; a non-releasable 'reserve pool', a 'readily releasable pool' (RRP) and an 'immediately releasable pool'. In conventional EM, thin (40-100 nm) sections are cut and imaged in two dimensions (2D) [4], [5]. The benefit of this technique is improved when combined with EM stereological techniques [6]. This combination of technique (spatial sampling based on small numbers of 2D images) has underpinned numerous morphometric studies to quantify changes in the Golgi structure [7], [8]. However, neither of these methods offers reliable insights into the three

dimensional (3D) detail or connectivity between the Golgi cisternae [9]. Thin sections from multiple cells and/or multiple regions from a single cell are unable to reveal the complete 3D organization of the Golgi and other structures involved in the secretory pathway [10]. Thus, this paper centered on developing improved methods for analyzing and characterizing variations in organelle morphology, particularly focus on insulin granule, based upon the semi-automated image processing and segmentation of sub-regions extracted from high resolution 3D image volumes generated using the technique of electron tomography (ET) and proposed a new hybrid method for quantification of meshed volume.

II. BACKGROUND: IMAGE FEATURES OF INSULIN GRANULES

Insulin granules are typically spherical and computationally easy to segment if the membrane is intact. In beta cells, there are predominantly two types of insulin granules: mature and immature [11]. In this study, this distinction has been ignored, thus only granule's general shape is focused while the insulin core is not be segmented. That being said, the position of the insulin core or crystal (relative to the granule membrane) plays a crucial role in determining the level of complexity.

Immature Granules

Immature granules can be either considerably larger or similar in size to mature granules but lack the well-defined insulin crystal core; instead, their uncleaved proinsulin cargo can be visualized as small punctate stain density of relatively uniform size and distribution within the granule lumen. Due to the fact that they appear less dense since the protein has not yet condensed in the granule core, immature granules are often called 'pale granules' [12], [13] in morphological studies due to this difference in stain density and can also exhibit more irregular shapes.

III. SUB-VOLUME EXTRACTION AND CLASSIFICATION

Insulin granules, one of the key cell compartments/organelles within the tomographic volumes were extracted using the *IMOD* software package [14]. Each of the sub-volume extracts was saved together with information such as volume size, mean density, minimum density and maximum density. Due to the variety of cellular compartment information as well as inherently high levels of background noise in the volumes, it was necessary to optimize

automated and semi-automated methods to segment these sub-volumes. This was initially done based on their ‘sub-group’. Each of these insulin granules sub-groups has discrete shapes, and sizes and differences in complexity. To further relate the simplified case scenarios for compartment structural complexity to actual examples drawn from the numerous tomograms generated by our group (Table 1). The actual data set examples used are incorporated into Figure 1.

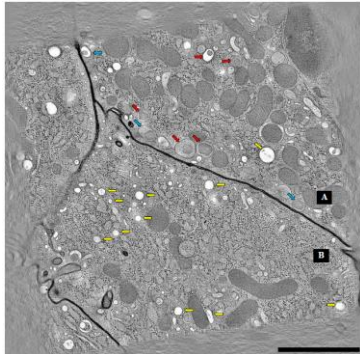


Figure 1: Dispersed location of insulin granules, yellow arrow shows immature insulin granules (Case 1), red and blue arrows show mature granules for Case 2 and Case 3 and/or Case 4, respectively. Label A and B represent different cell

Hybrid Meshing Quantification

Based on a 3D mesh contour of an object, its contour volume (CV) and mesh surface area (MSA) can be calculated and used for quantitative comparison with the manual reference set. Hybrid meshing quantification is introduced in this paper which integrates the CV followed by MSA. Meshing was performed automatically by using the *imodmesh* function in *IMOD*. The process was performed on the segmented stacks of image slices of each organelle. Accurate tracing results were then confirmed with the target scoring system [11].

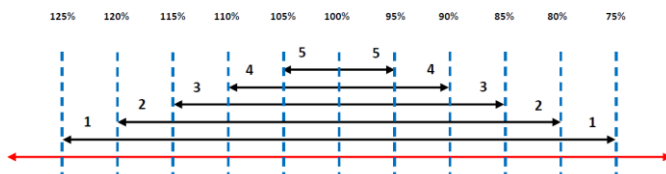


Figure 4: The target scoring system; 100% is referred as a target point of ground truth datasets. All mesh volumes of manual tracing is labelled as 100%. Any results of computational methods scored +/- 100% (of respective MSA) will determine a score of 5, and so on. Target scoring for each sub-group will differ according to its ground truth (gold standard) datasets. 5 scores of MSA range were proposed where 5 is the best while 1 is the worst [11]

i. Contour Volume (CV)

The contour volume (CV) is a sum of the area of contours (of each of Z slice of an object) times the distance to the connected contours in Z. The CV value is chosen for two reasons; 1) it handles the problem of skipped sections [14] and 2) it gives a slightly more accurate volume measurement for the capped regions because it integrates with a trapezoidal approximation [14].

$$(Area * Distance)_1 + (Area * Distance)_2 + \dots + (Area * Distance)_n \quad (1)$$

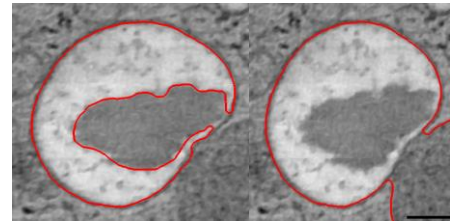


Figure 5: Two examples of failed (i.e. Score 2 or below) insulin tracing for insulin granule classified as Case 4. (left) Contour line traced broken insulin boundary (i.e. membrane). (right) The tracing contour excessively traced membrane attached to insulin membrane [11]. Scale bar: 100 nm

ii. Mesh Surface Area (MSA)

The mesh surface area is the total surface area of a mesh volume, computed by adding the areas of all the triangles in the mesh. In theory an object accurately segmented by two independent methods should have identical contour volumes. To test the effectiveness of contour volume (CV) as a metric to quantitatively compare contour sets of automated segmentation, they were assessed in comparison to a manual reference. By doing this, unwanted contour sets could be deleted in an automated manner when the CV value of automated segmentation did not closely match the CV of manually traced referenced contour sets. Furthermore this approach proved useful when more than one contoured volume was traced in a given tomographic sub-volume as the *mappick* function (*CoAn*) can be used to detect and delete unmatched volume(s). MSA, provide an exact measure of the area of the mesh, and was used as the second assessment of the segmentation results and for identification of the best combination of method settings.

$$(Area \text{ of triangle}) * (\text{Normal's Z component}) * (\text{Average of Z components of the triangle}) \quad (2)$$

By referring to the CV information of manual tracing contour set, unwanted objectmembranes were prevented from being traced to produce only the correct contour (Figure 2 and Figure 3). All mesh volumes of manual tracing is ‘labelled’ as 100%. Any results of computational methods scored +/- 100% (of respective MSA) will determine a score of 5, and so on. Target scoring for each sub-group will differ according to its ground truth (gold standard) datasets. 5 scores of MSA range were proposed where ‘5’ is the best while ‘1’ is the worst (Figure 4 and Figure 5).

IV. DISCUSSION AND FUTURE STUDY

With ongoing development of computational segmentation and visualization methods, e.g. image denoising algorithms, boundary- and region-based segmentation procedures, 3D image modelling methods etc., a high-fidelity cellular tomography segmentation pipeline – without any sacrifice of 3D surface model accuracy and employing only one single

parameter setting (i.e. parameter free) is very close to achievable/ accomplishable. Heavy noise and the unique characteristics of different organelles remain the persisting problems that influence segmentation accuracy with standard optimized settings.

A study on different segmentation methods including a number of image filtration and segmentation algorithms, different combination of those automated and semiautomated tracing processes and test of the efficiency of various mathematical morphology on 3D mesh surface models has yielded a new pipeline developed for the automated segmentation [11, 15]. Together with the newly proposed hybrid meshing quantification using contour volume followed by mesh surface area (MSA), a scoring system is developed [11, 15], and this pipeline has facilitated the study conducted here: to investigate the parameter optimization effectiveness on classified insulin granules. Overall, novel image classification and hybrid meshing quantification presented in this paper could have emerged that somehow would have outperformed the sum of previously existing computational algorithms. These tools could have led to novel biological findings.

The dataset collected here represents one of the most detailed analyses insulin granules in 3D. It therefore provides a useful reference set for classification of the organelles. Based on the experiments, there are significant findings established where more than 90% of more than 400 sub-volumes, that were sorted into sub-groups based on their respective image characteristic, were reported to have high-quality segmentation results (i.e. according to the MSA scoring they have scored between 5 to 3, i.e. a segmentation accuracy within +/- 15% of the manually traced/ground truth datasets). This demonstrates that the assigned standard sets of optimal parameter settings could be applied on particular organelle with respective/similar image characteristics. It also demonstrates the high quality of traced contours compared to the gold standard or reference contour set and improved the contour selection process for selecting the correct contour(s) and removed the unwanted contour(s) mathematically. This study has however brought to wider options of the studies in image segmentation, particularly insulin granules. While this paper has highlighted the research contribution, it is also discovered other way to (manually) classify insulin granules into its cases using the generation process of insulin secretion itself (Figure 6). This area of research is believed could be further analyzed and able to contribute for image processing studies.

ACKNOWLEDGMENT

The authors wish to thank Universiti Sains Malaysia for the support it has extended in the completion of the present research through Short Term University Grant No: 304/PKOMP/6313259.

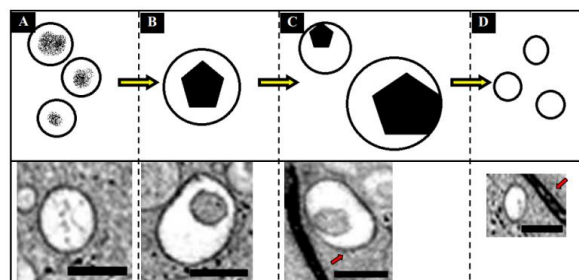


Figure 6: The changes of insulin granules from immature to mature granules in insulin secretion process (yellow arrow). From far left, immature insulin granules generates mature insulin core until this core merge to inner membrane and produce new (immature) granules (far right). Red arrow shows the cell membrane. Scale bar: 100 nm

REFERENCES

- [1] Olofsson, C. S., Salehi, A., Holm, C. & Rorsman, P., "Palmitate Increases L-Type Ca²⁺ Currents and the Size of the Readily Releasable Granule Pool in Mouse Pancreatic Beta- Cells," *Journal of Physiology*, vol. 557, pp. 935-948, 2004.
- [2] Hutton, J. C., "The Insulin Secretory Granule," *Diabetologia*, vol. 32, pp. 271-281, 1989.
- [3] Howell, S. L., "The Molecular Organization of the Beta Granule of the Islets of Langerhans," *Advances in Cytopharmacology*, vol. 2, pp. 319-327, 1974.
- [4] Ladinsky, M. S., Wu, C. C., Mcintosh, S., Mcintosh, J. R. & Howell, K. E., "Structure of the Golgi and Distribution of Reporter Molecules at 20 degrees C Reveals the Complexity of the Exit Compartments," *Molecular Biology of the Cell*, vol. 13, pp. 2810-2825, 2002.
- [5] Marsh, B. J., "Lessons from Tomographic Studies of the Mammalian Golgi," *Biochemical and Biophysical Acta*, vol. 1744, pp. 273-292, 2005.
- [6] Russ, J. C. & Dehoff, R. T., "Practical Stereology," *New York, Kluwer Academic/Plenum*, 2000.
- [7] Derganc, J., Mironov, A. A. & Svetina, S., "Physical Factors that Affect the Number and Size of Golgi Cisternae," *Traffic*, vol. 7, pp. 85-96, 2006.
- [8] Griffiths, G., Fuller, S. D., Back, R., Hollinshead, M., Pfeiffer, S. & Simons, K., "The Dynamic Nature of the Golgi Complex," *Journal of Cell Biology*, vol. 108, pp. 277-297, 1989.
- [9] Marsh, B. J., Mastronarde, D. N., Buttle, K. F., Howell, K. E. & Mcintosh, J. R., "Organellar Relationships in the Golgi Region of the Pancreatic Beta Cell Line, HIT T15, Visualized by High Resolution Electron Tomography," *Proceedings of the National Academy of Science U S A*, vol. 98, pp. 2399-406, 2001.
- [10] Ladinsky, M. S., Mastronarde, D. N., Mcintosh, J. R., Howell, K. E. & Staehelin, L. A., "Golgi Structure in Three Dimensions: Functional Insights From the Normal Rat Kidney Cell," *Journal of Cell Biology*, vol. 144, pp. 1135-1149, 1999.
- [11] Nur Intan Raihana, R., "Multiple, Object-oriented Segmentation Methods of Mammalian Cell Tomograms," *PhD Thesis*, The University of Queensland, 2014.
- [12] Rorsman, P. & Renstrom, E., "Insulin Granule Dynamics in Pancreatic Beta Cells," *Diabetologia*, vol. 46, pp. 1029-1045, 2003.
- [13] Noske, A. B., Costin, A. J., Morgan, G. P. & Marsh, B. J., "Expedited Approaches to Whole Cell Electron Tomography and Organelle Mark-up in situ in High-Pressure Frozen Pancreatic Islets," *Journal of Structural Biology*, vol. 161, pp. 298-313, 2008.
- [14] Kremer, J. R., Mastronarde, D. N. & Mcintosh, J. R., "Computer Visualization of Three-Dimensional Image Data using IMOD," *Journal of Structural Biology*, vol. 116, pp. 71-76, 1996.
- [15] Nur Intan Raihana, R., "Semi-automated Cellular Tomogram Segmentation Workflow (CTSW): Towards an Automatic Target Scoring System," *The International Conference on Computer Graphics, Multimedia and Image Processing*, 2014.

| Granule1 (total 49 contours) | Slice 10 | Slice 25 | Slice 40 | Comparison (3D visualisation) | Comments |
|------------------------------------|----------|----------|----------|----------------------------------|-----------------|
| Optimized M1 | | | | | Less acceptable |
| Optimized M2 | | | | | Less acceptable |
| Optimized M3 | | | | | Acceptable |
| Optimized M4 | | | | | Less acceptable |
| Optimized M5 | | | | | Acceptable |

Figure 2: Five examples of qualitative analysis from two significant 3D mesh results; *acceptable* and *unacceptable*. Cases that were classified as *acceptable* or *unacceptable* were based on comparison with manual tracing (*red contour line*) and the scoring system proposed in [11]

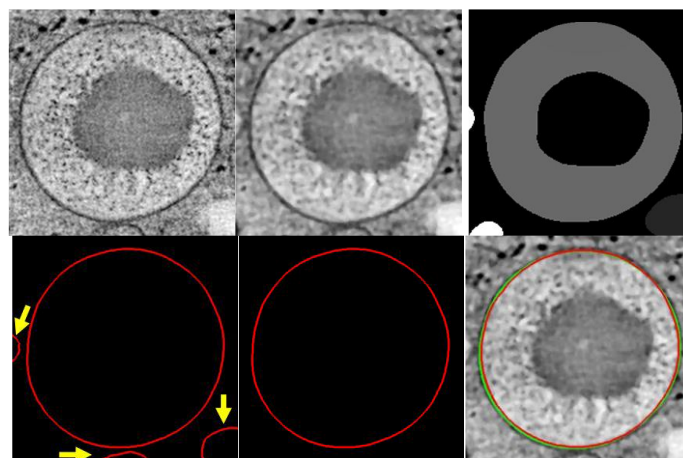




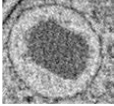
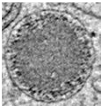
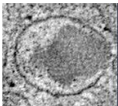
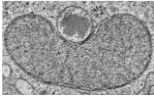


Figure 3: (*Upper row from left*) Original data of insulin granule classified for *Case 2*. (*middle*) Image was filtered using optimized non-linear anisotropic diffusion (NAD) filter. (*right*) Labelmap of filtered image using watershed segmentation. (*Lower row from left*) Contour lines generated from the label map image. Yellow arrows show extra contours also produced. (*middle*) Individual contour of insulin granule after all extra contours were deleted using information generated from contour volume (CV). (*right*) The final segmented contour using optimized parameter settings (*red contour*) on the background of the filtered image. It compares closely to the manually traced contour (*green contour*) [11]

Table 1
Cartoon images and real image data to represent different levels of complexity of granule ultrastructure

| | Case 1 | Case 2 | Case 3 | Case 4 |
|-----------------|--|--|--|---|
| Cartoon image |  |  |  |  |
| Real image data |  |  |  |  |
| Description | Singular/free in the cytoplasm. Throughout the reconstruction, empty lumen space separates the insulin core from the granule membrane. | Singular/free in the cytoplasm. Morphologically the same as Case 1, with one distinction: the granule lumen has varying degrees of staining density. | Singular/free in the cytoplasm. The insulin crystal contacting (or appearing to contact) the granule membrane. | Proximal to, or in (apparent) contact with other organelles/ compartments |